frontiers | Frontiers in Marine Science

TYPE Original Research
PUBLISHED 03 November 2022
DOI 10.3389/fmars.2022.963193

OPEN ACCESS

EDITED BY
Chen-Tung Arthur Chen,
National Sun Yat-sen University,
Taiwan

REVIEWED BY
Qianguo Xing,
Yantai Institute of Coastal Zone
Research (CAS), China
Francisco Arenas,
University of Porto, Portugal

*CORRESPONDENCE
Kitack Lee
ktl@postech.ac.kr

SPECIALTY SECTION
This article was submitted to
Coastal Ocean Processes,
a section of the journal
Frontiers in Marine Science

RECEIVED 07 June 2022
ACCEPTED 30 September 2022
PUBLISHED 03 November 2022

CITATION
Kim J-M, Lee K, Han I-S, Kim M,
Kim J-H, Kim T-H, Kim H, Jeon BH
and Shin K (2022) Factors governing
seawater carbonate dynamics in a
macroalgal habitat.
Front. Mar. Sci. 9:963193.
doi: 10.3389/fmars.2022.963193

Factors governing seawater carbonate dynamics in a macroalgal habitat

Ja-Myung Kim[1], Kitack Lee[1,2]*, In-Seong Han[3], Miok Kim[1], Ju-Hyoung Kim[4], Tae-Hoon Kim[5], HyunKyum Kim[6], Byung Hee Jeon[6] and Kyoungsoon Shin[7]

[1]Division of Environmental Science and Engineering, Pohang University of Science and Technology, Pohang, South Korea, [2]Institute for Convergence Research and Education in Advanced Technology, Yonsei University, Seoul, South Korea, [3]Ocean Climate and Ecology Research Division, National Institute of Fisheries Science, Busan, South Korea, [4]Department of Aquaculture and Aquatic Science, Kunsan National University, Gunsan, South Korea, [5]Department of Oceanography, Chonnam National University, Gwangju, South Korea, [6]Ecological Restoration Division, Korea Fisheries Resources Agency, Busan, South Korea, [7]Ballast Water Research Center, Korea Institute of Ocean Science and Technology, Geoje, South Korea

Photosynthetic organisms shift the dynamics of surface pCO_2 driven by the sea surface temperature change (thermodynamic driver) by assimilating inorganic C from seawater. Here we measured net C uptake in a macroalgal habitat of coastal Korea for two years (2019-2020) and found that the macroalgal habitat contributed 5.8 g C m^{-2} $month^{-1}$ of the net C uptake during the growing period (the cooling period, September–May). This massive C uptake changed the thermodynamics-driven seasonal dynamics such that the air–sea equilibrium of pCO_2 was pushed into disequilibrium. The surface pCO_2 dynamics during the cooling period was mostly influenced by the seasonal decrease in temperature and the proliferation of macroalgae, while the dynamics during the warming period (the stagnant period, June–August) closely followed that predicted based solely on the change in sea surface temperature (thermodynamic driver). In contrast to the phytoplankton-dominated offshore waters (where phytoplankton populations are large in spring and summer), the impact of coastal macroalgae on surface pCO_2 dynamics was most pronounced during the cooling period, when the magnitude of pCO_2 change was as much as twice that resulting from temperature change. Our study shows that the distinctive features of the macroalgal habitat—in particular the seasonal temperature extremes (~18°C difference), the active macroalgal metabolism, and anthropogenic nutrient inputs—collectively influenced the seasonal decoupling of seawater and air pCO_2 dynamics.

KEYWORDS

coastal ocean carbon, biological community metabolisms, diel carbon dynamics, East Sea, air-sea CO_2 flux, macroalgal habitat, seaweed habitat

Introduction

Decades of research on the ocean carbon cycle have improved our understanding of the mechanisms underlying variations of seawater carbonate (C) parameters in diverse ocean regimes. Seasonal variations in ocean temperature largely determine the pCO_2 distributions in the open ocean. Another key process is air-sea CO_2 exchange, which substantially reduces the temperature-induced air-sea disequilibrium. Consequently, the rate of pCO_2 increase in the open ocean is broadly consistent with the rate of increase in atmospheric pCO_2, although episodic biological activity and lateral and vertical mixing still act to induce the air-sea pCO_2 disequilibrium (Takahashi et al., 2006; Takahashi et al., 2009).

In contrast to the factors controlling carbonate dynamics in the open ocean, various processes (e.g., wind-driven upwelling, freshwater input, eutrophication, massive biological production and respiration) complicate the dynamics in coastal environments (Borges, 2011; Cai et al., 2011; Kim et al., 2020; Li et al., 2022). A study using a global C database showed that the latitudinal distributions and seasonality of global coastal surface pCO_2 are regulated by nonthermal factors (i.e., water mixing and net primary production) (Laruelle et al., 2017). Moreover, Cai et al. (2020) reported on the comparative effects of different drivers (i.e., upwelling and biological production) on the local variability of pCO_2 in a range of domains along North American ocean margins. Other studies in the South China Sea revealed distinctive differences between ocean-dominated and river-dominated ocean systems (Cao et al., 2019).

In particular, the processes occurring in coastal environments act in concert to increase phytoplankton biomass: pico- and microalgae (phytoplankton) in off-shore waters; phytoplankton and macrophytes (including macroalgae and angiosperm species) in nearshore waters. To assess the biological influence on the coastal carbonate dynamics, studies to date have examined the biological contribution to air–sea CO_2 fluxes at individual coastal systems and diagnosed the CO_2 source and sink nature of the coastal oceans (Dai et al., 2013; Laruelle et al., 2014). Despite the diverse dependency of the C flux on the biological productivity and disparities in air–sea CO_2 fluxes at regional scales (Signorini et al., 2013; Gruber, 2015; Kubo et al., 2017), nearshore macroalgal habitats (occupying ~3.5 million km^2 globally) were identified as an important CO_2 sink (Ikawa and Oechel, 2015; Krause-Jensen and Duarte, 2016; Watanabe et al., 2020). Globally, the macroalgal habitats account for a net primary production of 1020–1960 Tg C yr^{-1} and thus have the potential to export of 61–268 Tg C yr^{-1} (Krause-Jensen and Duarte, 2016). By comparison, blue carbon (referring to organic C sequestered by seagrass meadows, tidal marshes, and mangrove forests) was reported to account for a maximum annual organic C burial rate of 329 Tg C yr^{-1} globally (Nellemann et al., 2009; Macreadie et al., 2019). A thorough mechanistic understanding of the biological contribution is urgently needed to fully characterize the C dynamics in the macroalgal ecosystems (Duarte et al., 2022).

We here assess the significance of biological control in regulating the dynamics of the carbonate parameters—pCO_2, pH, C_T (total dissolved inorganic carbon), and Ω_{arag} (the seawater calcium carbonate saturation state with respect to aragonite)—in a productive macroalgal habitat of Korea. We highlight the extreme dynamics of surface water pCO_2, which can represent productive nearshore ecosystems with natural and anthropogenic forcings (including large seasonal temperature variations, biological community metabolism, and anthropogenic nutrient inputs). We also provide a framework that explains the thermodynamically driven variations of carbonate parameters to facilitate data interpretation. These parameters include continuous time-resolved (1-h intervals) carbonate parameter measurements using an autonomous pCO_2 sensor and discrete (weekly intervals) measurements for the two year period (2019–2020). Using these observations of carbonate parameters, we further explore the sensitivities of individual carbonate parameters to changes in the major environmental factors in the macroalgal habitat.

Materials and methods

Survey data

The study site was a shallow macroalgal habitat (36.154°N, 129.401°E) bound by tidal barriers in the East Sea (Figures 1A, B), in which carbonate chemistry has been well characterized in terms of seasonality and locality (Park et al., 2006; Lee et al., 2011). Surface-water pCO_2 was continuously measured using an autonomous pCO_2 system (Supplementary Text 1) from January to September in 2019 and from March to December in 2020. The pCO_2 mooring system was anchored to the bottom of the macroalgal habitat (10 m depth; dominated by canopy forming species (e.g., *Ecklonia cava*, *Sargassum horneri*, *Saccharina japonica* and understory species; Figure 1C), and the pCO_2 sensor package was submerged ~0.5 m below the surface. Surface-water pCO_2 (or pH), temperature and salinity were measured at 1-h intervals for the entire period of 2019–2020.

During the observation period, we also collected discrete surface samples for seawater carbonate parameters—pH, A_T (total alkalinity), and C_T—and nutrients (NO_3^-, HPO_4^{2-} and Si $(OH)_4$) at 3–4 d intervals (the number of samples = 184). The chosen parameters were determined using spectrophotometry for pH (Clayton and Byrne, 1993; Lee et al., 1996), and using potentiometric and coulometric titration for A_T and C_T, respectively, and using colorimetry for nutrients (Zhang et al., 2001) (Supplementary Text 1).

For comparison, off-shore waters in the vicinity of the macroalgal habitat were sampled for the measurement of A_T and

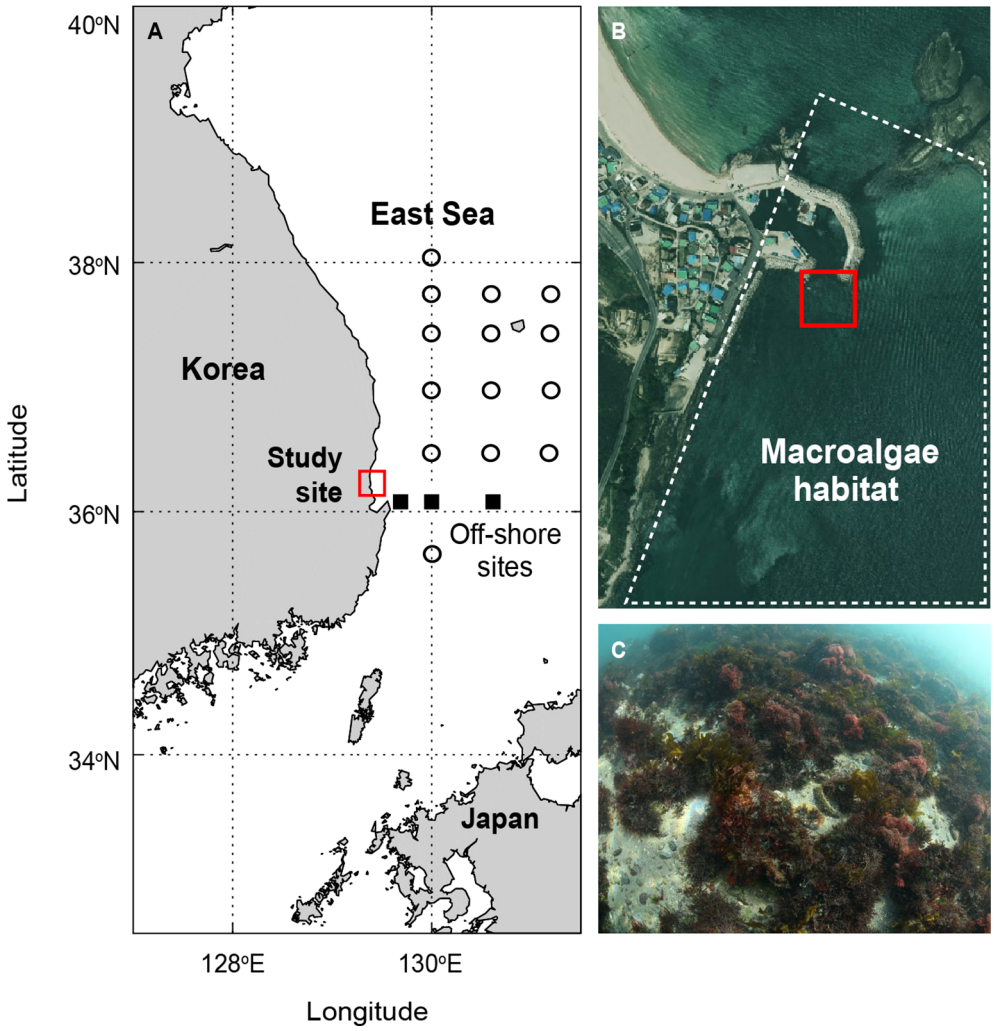

FIGURE 1
(A, B) Sampling site of this study (red box), and **(C)** dominant macroalgal species in the habitat. The off-shore sites in **(A)** indicate the location of the sampling site dominated by microalgae for comparison. The seawater carbonate data measured at three sampling stations (squares) in the off-shore sites were used to estimate the effects of off-shore water intrusion.

C_T at 17 hydrographic stations in the East Sea (Figure 1A) in February, April, August, and October 2019–2020, as part of the National Institute of Fisheries Science Serial Oceanographic Observation project. For each sample, the salinity, temperature, and nutrient concentrations were measured.

Carbonate parameters

For the continuous measurements, the values for seawater carbonate parameters—pH, C_T, and Ω_{arag}—at *in situ* conditions ($C_{in\ situ}$) were calculated from the measured values of pCO_2 and A_T (interpolated from the discrete A_T values) (Dickson et al., 2007) using the CO2SYS program applying the carbonic acid dissociation constants of Mehrbach et al. (1973) (as refitted into different functional forms by Dickson and Millero, 1987), the total boron-molality-to-chlorinity ratio reported by Lee et al. (2010), and other ancillary constants tabulated by Millero (1995). This group of input parameters and thermodynamic constants yielded the errors of ±0.003 pH, ±2.3 μmol kg^{-1} C_T, and ±0.02 Ω_{arag}. For the discrete and off-shore seasonal measurements, we used the pair of C_T and A_T to calculate the $C_{in\ situ}$ because direct measurements agreed with calculations (Lueker et al., 2000; Fong and Dickson, 2019).

C flux and uptake by biology

Net air–sea C fluxes were determined using the formula of flux (mol C $area^{-1}time^{-1}$) = $K_0 \cdot k(pCO_2^{air} - pCO_2^{sw})$, where K_0 (mol L^{-1} atm^{-1}) is the CO_2 gas solubility (Weiss, 1974) and k

(cm hr^{-1}) is the gas transfer velocity (= $0.251 \cdot U_{10}^2$ $(Sc/660)^{-0.5}$, where U_{10} (m s^{-1}) is the windspeed at 10 m above sea level, and Sc is the Schmidt number (Wanninkhof, 2014). A positive value of the resulting flux represents C sink; *vice versa*, C source. Daily mean pCO_2^{air} (μatm) data were obtained from Ulleung observatory (37.48°N, 130.90°E). Hourly mean windspeed data for estimating U_{10} at the sampling site were measured in the vicinity of the macroalgal habitat (36.35°N and 129.78°E).

The amounts of C_T uptake by biology (C_T^{bio}) were computed from the rate of C_T changes after the C_T values were normalized to an annual mean salinity (nC_T in the unit of μmol C kg seawater^{-1} = $C_T \times S_{MEAN}/S_{IN\ SITU}$, where S_{MEAN} and $S_{IN\ SITU}$ are the annual mean and *in situ* salinity values, respectively) (Supplementary Figure 1A) and corrected for the effects of off-shore water intrusion (Supplementary Text 2) and the total C changes *via* $flux^{air-sea}$ (mol C mass of seawater^{-1}time^{-1} = $K_0 \cdot k(pCO_2^{air} - pCO_2^{sw})(density)^{-1}(water\ depth)^{-1}$) during the period of analysis (C_T^{bio} = *−the rate of* nC_T *changes corrected for the effects of off–shore water intrusion* × *time* + ΣC *changes via* $flux^{air-sea}$). The annual net C_T^{bio} was calculated as the sum of C_T^{bio} values measured for the growing (photosynthesis dominant) and stagnant (respiration active) periods. The division between the growing (cooling; September –May) and the stagnant (warming; June–August) periods was made based on the temporal changes in nitrate concentration reflecting consumption (a decrease in concentration) and regeneration (an increase in variability) (Supplementary Figure 1B). In addition, seasonal variations in the net primary production (NPP), showing a rapid decrease starting from June (personal communication) because of a decrease in algal biomass, were used as criteria for dividing the periods.

Calculations of pCO_2 changes arising from changes in seawater temperature, biology, and net air–sea C flux

Changes in the seawater carbonate parameters arising from changes in the sea surface temperature (SST) (C_{temp}) were thermodynamically calculated using the experimentally determined pCO_2–SST relationship of 4.23% pCO_2 change °C^{-1} (Lee and Millero, 1995; Takahashi et al., 2002). The pair of A_T and $pCO_{2\ temp}$ (= annual mean $pCO_2 \times \exp[0.0423\ (SST_{IN\ SITU} - SST_{MEAN})]$) were used as input parameters to CO2SYS at $SST_{IN\ SITU}$. To calculate the equilibrium values of the seawater carbonate parameters (C_{eq}, assuming pCO_2^{sw} is fully equilibrated with pCO_2^{air}), the pair of A_T and pCO_2^{air} (= pCO_2^{sw}) were used instead.

The monthly cumulative changes in pCO_2 arising from changes in temperature, biology, and air–sea C flux were estimated on an hourly basis from the beginning of each month ($\Delta pCO_{2t=0}$; t=0, at midnight of the first day of each month). Analogously, the accumulated changes in pCO_2 during the cooling and warming periods were calculated on a monthly basis from the beginning month of the period (t=0, the monthly mean of September and June, respectively) as follows:

$$\Delta net = pCO_2^n - pCO_{2t=0} \quad (1)$$

$$\Delta temp = pCO_{2t=0} \cdot exp[0.0423(SST^n - SST_{t=0})] \quad (2)$$

$$\Delta bio = \Delta net_{flux\ corr} - \Delta temp \quad (3)$$

$$\Delta flux = \Delta net - \Delta net_{flux\ corr} \quad (4)$$

where Δnet, Δtemp, Δbio, and Δflux are the accumulated changes of pCO_2 resulting from the effect of all factors (i.e., measured changes), temperature, biology, and C flux, respectively, and $\Delta net_{flux\ corr}$ is the cumulative change in pCO_2 after removing the influence of C flux. To obtain this value, the flux corrected pCO_2 was estimated using a model calculation with an input pair of A_T and $C_{T\ flux\ corr}$ (= $C_T^n - \sum_{t=0}^{n}$C changes *via* $flux^{air-sea}$).

Results and discussion

Dynamics of carbonate parameters and the amounts of C uptake by the macroalgal habitat

For 2019–2020, seasonal variations in air temperature over the East Sea resulted in a 17.5°C seasonal amplitude in the SST (Figure 2A). Much of the net increase in surface pCO_2 during the warming period (the stagnant period, June–August) was driven by temperature elevation (Figures 2B, C), whereas the pCO_2 decrease during the cooling period (the growing period, September–May) was attributed more to the combined effects of decreasing temperature and the net growth of dominant macroalgal species (See Discussion below). The seawater pCO_2 values being lower than the atmosphere level (~80 μatm) during this period resulted in the influx of atmospheric C (220 μmol C_T kg^{-1}) into the macroalgal habitat (Figure 2D and Supplementary Figure 2B). The net C_T uptake by the macroalgal habitat (C_T^{bio}) was found to be 4.4 g C m^{-2} $month^{-1}$ in the cooling period (Supplementary Table 1). This C_T^{bio} value was further corrected for the effects of lateral intrusion of off-shore water using the residence time of water at the study site (10 days; Park et al., 2015) and seasonal changes in off-shore water nC_T. The revised C_T^{bio} was then increased to 5.8 g C m^{-2} $month^{-1}$ (See details in Supplementary Table 1, Supplementary Text 2 and Supplementary Figure 3). During the cooling period, dissolved inorganic C was assimilated into macroalgae bodies (transforming into particulate organic C) at a rate of 22.5 μmol kg $seawater^{-1}$ $month^{-1}$ (Supplementary Figure 2A), whereas only a fraction of the assimilated C was slowly released in dissolved form, with a net increase of 6.6 μmol kg $seawater^{-1}$ $month^{-1}$ in seawater during the later months of this period (from February to May) (Supplementary Figure 2C). Subsequently, the concentration of dissolved organic C

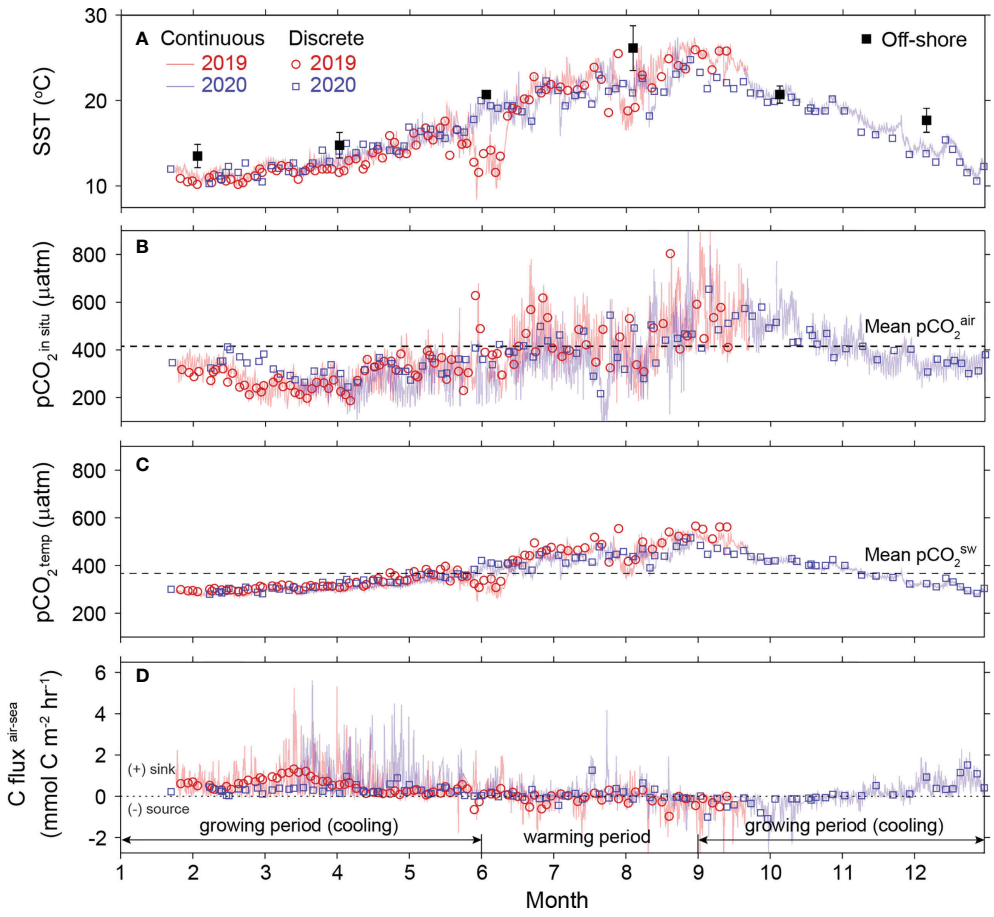

FIGURE 2
Temporal changes in **(A)** sea surface temperature (SST), **(B)** seawater pCO_2, **(C)** seawater pCO_2 arising from SST change only, and **(D)** air-sea C flux for the period 2019–2020. Lines and open symbols indicate the continuous and discrete data, respectively, obtained in 2019 (red) and 2020 (blue). Solid symbols (black) in **(A)** represent the seasonal changes in off-shore SST. Horizontal line in **(B, C)** show the level of mean pCO_2 of the air (415 µatm) and seawater (367 µatm), respectively.

during the warming (stagnant growth) period increased with that of nC_T at a similar rate of 14.6 µmol kg seawater^{-1} month^{-1}. Compared with the varying dynamics of pCO_2 (i.e., changes in pH mirroring pCO_2; Supplementary Figure 1C), the variation of C_T was not strongly affected by the seasonal temperature changes (Supplementary Figure 1D). The seasonal variation of Ω_{arag} was relatively constant (with an annual mean value of 2.6 ± 0.4; Supplementary Figure 1E).

The annual net C uptake of 48 g C m^{-2} yr^{-1} (C_T^{bio}) represents the C_T utilization by all biological communities at the study site, and thus corresponds to the net community production (NCP, defined as the difference between net primary production of autotrophs and respiration of heterotrophs) (Supplementary Table 1). Therefore, the estimated C_T^{bio} is lower than the NPP (C assimilated only by autotrophs *via* photosynthesis, excluding net ecosystem primary production) values reported for other macroalgal habitats: for example, annual mean NPP values of 910 g C m^{-2} yr^{-1} and 1270 g C m^{-2} yr^{-1} for *Ecklonia cava* and *Saccharina japonica*-dominant habitats in Japan, respectively (Nakawaki et al., 2001; Tominaga et al., 2004); 90–490 g C m^{-2} yr^{-1} for *Sargassum horneri*-dominant habitats in Korea (Choi et al., 2020); and a global mean of 273 g C m^{-2} yr^{-1} for total rocky habitats (Duarte et al., 2022). Moreover, the thermal stress on algal metabolism in summer accelerated the transformation of organic C to CO_2, thereby lowering the net C uptake by the macroalgal habitat investigated here. This is another factor causing our C uptake value to be lower than the values in the literature.

Temperature dependence of carbonate parameters

Variations in seawater temperature are the primary driver of the dynamics of carbonate parameters in the surface ocean

because they control the acid-base equilibria in seawater (Weiss, 1974; Lueker et al., 2000; Zeebe and Wolf-Gladrow, 2001) (Supplementary Text 3). In a closed system, without air-sea CO_2 exchange (the red solid lines in Figure 3 and Supplementary Figure 4), an increase in temperature rapidly increases the level of pCO_2 but lowers the pH, whereas it does not change the C_T—the total C concentration which is not altered by the speciation changes of individual carbonate species. The temperature increase contributed to a minor increase in the Ω_{arag} when the salinity, C_T, and A_T remained unchanged. In a hypothetical open system, by contrast, which instantaneously reaches the full equilibration of seawater pCO_2 with the atmospheric pCO_2 (the black solid lines in Figure 3), the seawater pCO_2 (to which pH directly correlates) did not increase with increasing temperature, largely because of the complete compensation for changes in C *via* CO_2 efflux, further decreasing C_T but increasing carbonate ion concentration ($[CO_3^{2-}]$, which is directly proportional to Ω_{arag}). The dynamics of *in situ* carbonate parameters at the macroalgal habitat did not entirely follow the two trends predicted by either temperature change or the full equilibrium with respect to the atmospheric pCO_2 *via* infinitely fast C exchange. However, the observed trends of carbonate parameters as functions of temperature were explicitly closer to the dynamics expected for a closed system. Our finding is solid evidence that the air-sea C flux was not sufficiently large to completely offset the air-sea disequilibrium of pCO_2.

Biological activities altering temperature-driven carbonate dynamics

Large deviations (colored circles in Figure 3) of the C parameters from the thermodynamic estimation (the solid red lines) indicate that factors other than temperature (i.e., biological activities and air-sea C flux) were also the key driver of the carbonate dynamics in the macroalgal habitat. We highlight the changes in daily extreme carbonate parameters (the maximum and minimum) associated with the non-thermal processes in plots (Figure 4 and Supplementary Figure 5) by showing changes in the *in situ* carbonate parameters ($C_{in\ situ}$) against those of the same parameters arising solely from the temperature change (C_{temp}) (Figures 4A–D), and in plots showing the differences between $C_{in\ situ}$ and C_{temp} against months or hours (Figures 4E–H). Both *in situ* values of pCO_2 and pH generally followed the 1:1 trends with $pCO_{2\ temp}$ and pH_{temp}, with considerable deviations from $pCO_{2\ temp}$ and pH_{temp} (Figures 4A, B). By contrast, the values of $C_{T\ temp}$ and $\Omega_{arag\ temp}$ showed narrow dynamic ranges, which were attributed primarily to the insensitivities of C_T and lower sensitivity of Ω_{arag} to changes in temperature (Supplementary Text 3). The dynamic range of $C_{T\ temp}$ was greater than that of $\Omega_{arag\ temp}$ because some of the variations in $C_{T\ temp}$ in our study site were caused by variations in $A_{T\ in\ situ}$, but not by variations in temperature (Figures 4C, D).

To confirm that the deviations of $C_{in\ situ}$ from C_{temp} (observation – calculation) mostly originated from biological metabolisms—photosynthesis and respiration—we plotted the daily extreme offsets of the four carbonate parameters measured continuously at 1-h intervals against months (x-axis) or hours (red dots for the time window for respiration dominant and blue dots for photosynthesis dominant) (Figures 4E–H). Most of the extreme offsets were observed at hours when the dissolved oxygen concentration (a good indicator of primary production and respiration of biology) reached the daily maxima or minima (Supplementary Figure 6), albeit with a lag of a few hours arising from for influence of metabolisms on the carbonate chemistry to be fully accumulated in the water column.

Contributions of key factors to seawater pCO_2 variations

Factors responsible for the dynamics of pCO_2 in the macroalgal habitat include temperature, biological activities, and C flux at the air–water interface. The monthly contribution of each factor to $pCO_{2\ in\ situ}$ variations was highly variable over months and occasionally changed the sign (Figure 5). The contribution of temperature variations was more pronounced in summer and late fall (50–60%); however, their monthly contribution (17%) was, on average, only one-third of the contributions of biology or three-quarters the contributions of the air–sea C flux each month. The contributions of biology and the air–sea C flux were generally pronounced throughout the year.

During the cooling period (the growing period, September –May), the net accumulated change in pCO_2 was primarily associated with the seasonal decrease in seawater temperature and the proliferation of macroalgae (Figures 6A–C). For most of the cooling months the contribution to pCO_2 change resulting from seawater temperature change (%Δtemp) was greater than that driven by other factors. The pronounced seasonal temperature effect on pCO_2 appeared to be ubiquitous in the coastal waters around Korea (Lee et al., 2022). However, the contribution of temperature change became smaller than the biological contribution (%Δbio) in the latter growing months, as the macroalgal growth remained strong. At the end of the growing season, Δbio was a factor of three greater than the net non-thermal changes (= the differences between Δnet and Δtemp). During the warming period (the stagnant period, June –August) (Figures 6D–F), the net accumulated change (Δnet) approximately followed the Δtemp, with negligible net contributions from non-thermal factors.

Contrary to the non-thermal pCO_2 change in the phytoplankton-dominated off-shore waters (the inset in Figure 6A), the non-thermal change observed in the macroalgal habitat (primarily driven by the biological production) was maximal during the cooling period. This

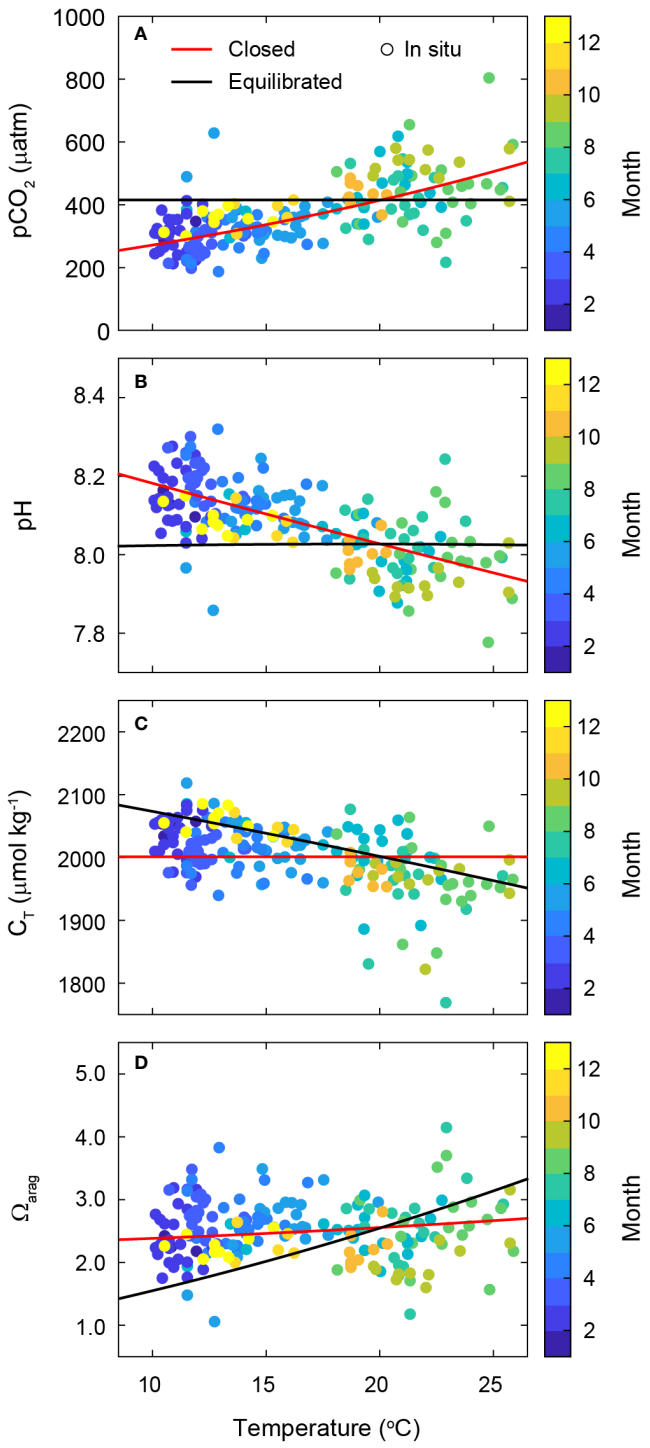

FIGURE 3
Temperature dependence of seawater carbonate parameters: **(A)** pCO_2, **(B)** pH, **(C)** C_T, and **(D)** Ω_{arag}. Thermodynamic changes with varying temperature in the closed system (red lines) are calculated at the constant values of C_T (2001.9 µmol kg^{-1}), A_T (2239.2 µmol kg^{-1}), and salinity (33.5), which were the mean concentrations of the discrete measurements. Theoretical changes in the equilibrated system (black lines) are estimated under the assumption of complete equilibration of pCO_2^{sw} with pCO_2^{air} (415.0 µatm) (with the constant A_T of 2239.2 µmol kg^{-1}). Colored circles overlaid by month indicate the measured values of carbonate parameters at *in situ* conditions during the discrete measurements (2019–2020).

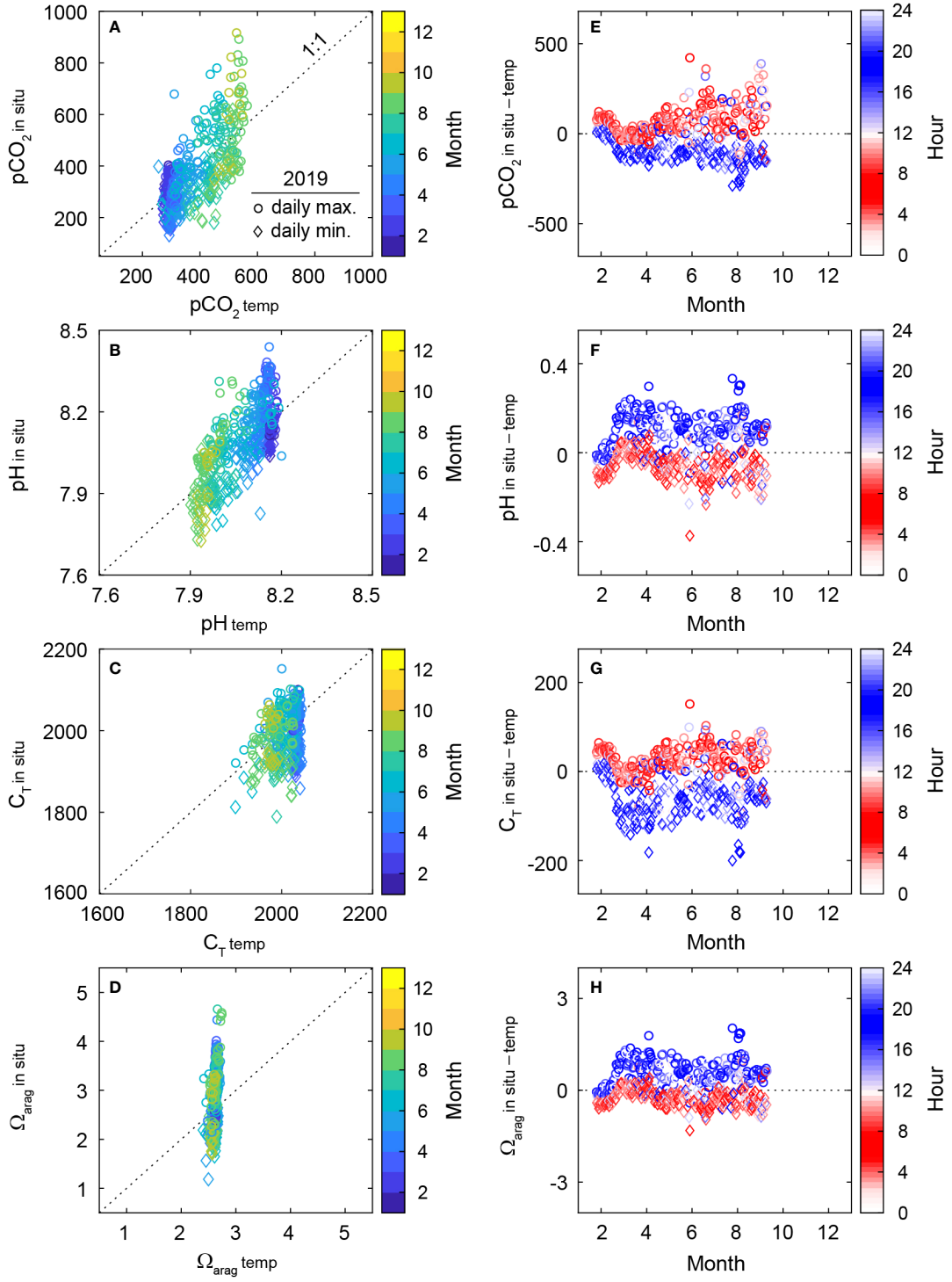

FIGURE 4
(A–D) Relationship between the *in situ* carbonate parameters ($C_{in\ situ}$) obtained during the continuous measurements and the parameters resulted from the change of temperature (C_{temp}: calculated from the estimated pCO_2 based on thermodynamic shifts in the closed system and A_T under the *in situ* conditions). Only the daily extremes (circles: maximum; diamonds: minimum) observed in 2019 are displayed to conserve space with a color-coding by month. **(E–H)** The daily extreme differences between $C_{in\ situ}$ and C_{temp} during the continuous measurements in 2019. The color of the symbols overlaid by the time of measurement. The data for the year 2020 is shown in Supplementary Figure 5.

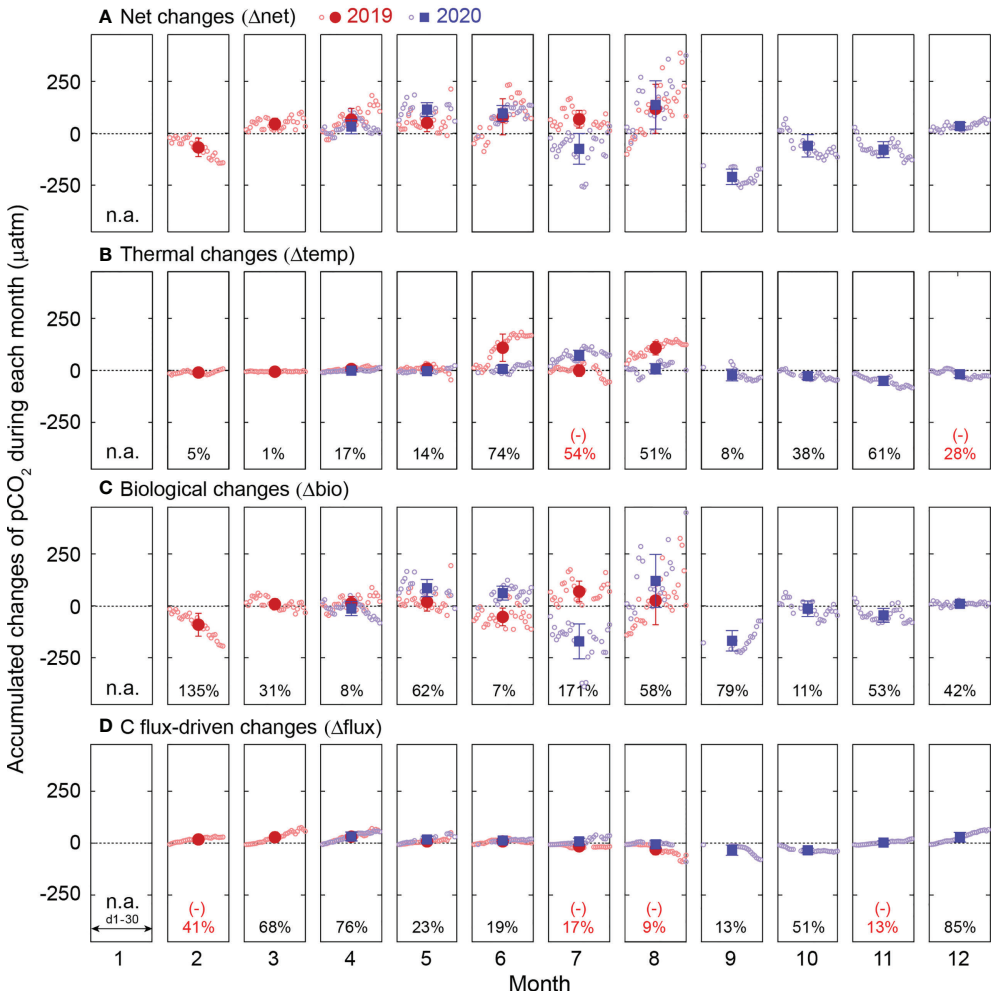

FIGURE 5
The monthly accumulated changes in pCO_2 from the beginning of each month driven by **(A)** all factors (Δnet), **(B)** temperature (Δtemp), **(C)** biological activity (Δbio), and **(D)** C flux (Δflux) during the continuous measurements in 2019 (red) and 2020 (blue). Open circles represent the accumulated hourly changes of pCO_2. Filled symbols and error bars indicate the monthly mean values of the accumulated hourly changes during a month and the standard deviation of the daily means, respectively. The relative contribution (%) of each factor was derived from the proportion of the calculated two-year monthly mean value to that of the Δnet. Negative values (numbers in red) indicate the opposite direction of change to the Δnet. n.a. indicates 'data not available'.

difference was caused by the temperature-dependent metabolic rate of macroalgae, which generally have an optimum growth temperature condition of 7–17°C in case of canopy forming species (Fortes and Lüning, 1980; Serisawa et al., 2003; Skriptsova et al., 2004; Gao et al., 2017). Exposure to temperatures higher than those optimal for growth, the macroalgal bodies tended to disintegrate into dissolved organic matter. Factors involved in maintaining macroalgal structure (turgidity, vacuoles, and plasmolysis) deteriorate considerably under thermal stress (> 20°C) (Kakinuma et al., 2006), (Supplementary Figure 7).

Correlation between seawater pCO_2 *in situ* and atmospheric pCO_2

The impacts of major controlling factors on the sign and magnitude of pCO_2 variations differ in different ocean regimes and time scales (diel to annual). In most ocean environments, the seasonal seawater temperature variations are primary deriver of surface pCO_2 changes; therefore, the seasonal temperature extremes (ΔSST) would strongly affect the overall directions. When the $pCO_{2\ in\ situ}$ values were correlated to the pCO_2^{air} (low in summer and high in winter due to photosynthesis and respiration of the terrestrial

10.3389/fmars.2022.963193

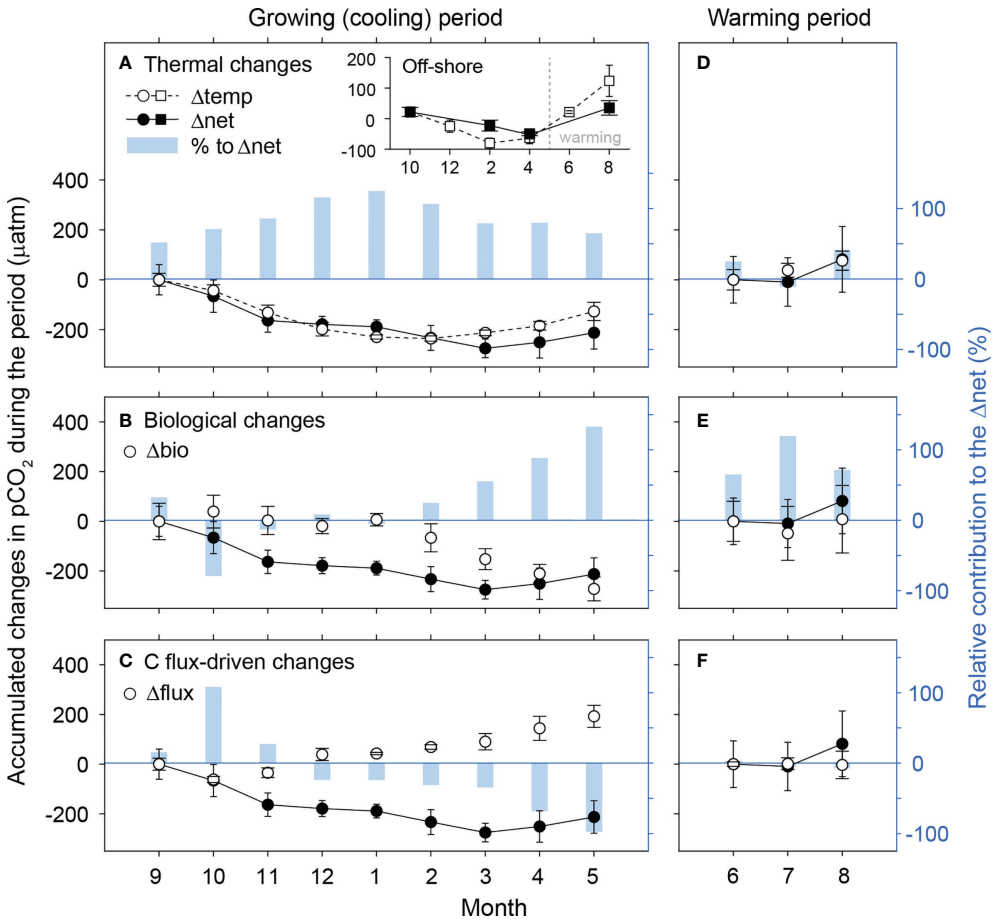

FIGURE 6
Accumulated changes in pCO_2 during **(A–C)** the cooling and **(D–F)** the warming periods (2019–2020) from the first month of each period (September and June, respectively), driven by temperature (Δtemp; **A**, **D**), biological activity (Δbio; **B**, **E**), and C flux (Δflux; **C**, **F**). Solid symbols indicate the changes resulting from all factors (Δnet). The right y-axis shows the relative contribution (%) of each factor to Δnet. Negative values indicate the opposite direction of change to the Δnet. Inset: Δtemp and Δnet for off-shore waters along the latitude 36.08°N (129.69, 130.00 and 130.62°E) over the cooling and warming periods from October (2019–2020).

ecosystem, respectively), negative correlations (i.e., the seasonal decoupling between air *versus* seawater pCO_2 variations) were common in diverse ocean regions but considerably varied: −11.9 in our in-shore macroalgal habitat (18°C ΔSST), −5.6 in the off-shore water (13°C ΔSST), and −1.2 in the open ocean (5°C ΔSST), respectively (Figures 7B–D). The slopes (i.e., the magnitude of seasonal difference between air *versus* seawater pCO_2) found in the studied macroalgal habitat were much steeper than those found in the Hawaii Ocean Time-series site, where seasonal temperature changes are small. Because the biological activity can lead to the deviation of the surface pCO_2 dynamics, the magnitude of deviation from the temperature-governed slope was more prominent in productive environments: the macroalgal habitat (where both micro-and macroalgae dominant) > off-shore (microalgae dominant) > open ocean (low biomass); Figure 7.

In the absence of strong temperature and biology effects, the air–sea C flux would eventually remove the air–sea pCO_2 disequilibrium in decadal time scales. However, on a seasonal scale the CO_2 gas exchange is not fast enough to fully compensate for the seawater pCO_2 changes caused by multiple factors. The air–sea C flux would contribute to the relationship between $pCO_{2\ in\ situ}$ and pCO_2^{air} (yielding a 1:1 trend) on a decadal scale by shifting the observed seasonal trends upward over the years, specifically in the regions where the effects of other controlling factors are marginal (gray circles in Figure 7D). Contrarily, the dynamics of surface pCO_2 in our study site—reflecting the additional features of a nearshore ecosystem, such as the influence of increasing loads of anthropogenic nutrients—were reinforced by high biological activity. Our 2 year observations are not sufficient to estimate inter-annual

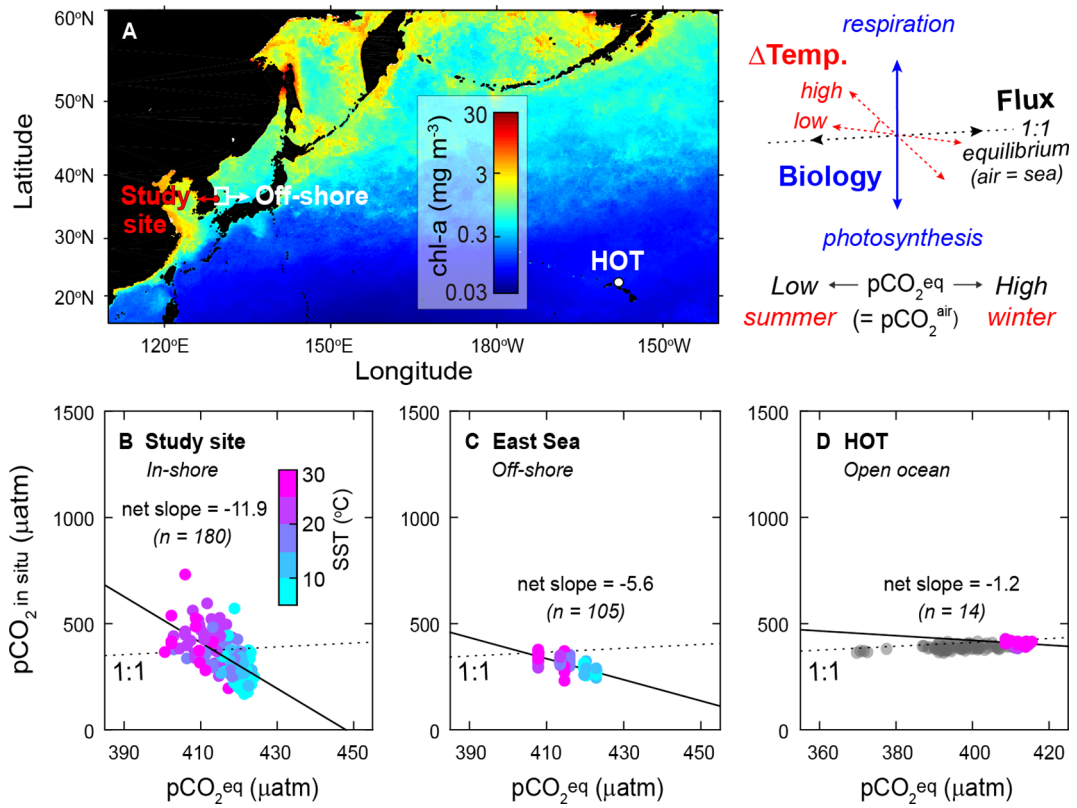

FIGURE 7
(A) Distribution of the annual mean chlorophyll-a concentration of 2019 in the northwestern Pacific Ocean, **(B–D)** correlations between the fully equilibrated pCO_2 with atmospheric CO_2($pCO_{2\,eq}$ = pCO_2^{air}) and *in situ* seawater pCO_2 measured in the regions with different seasonal temperature extremes and biological activities: **(B)** the macroalgal habitat (plotted data were obtained during the discrete measurements during 2019–2020; r^2 = 0.403, p = 1.1 ×10^{-21}), **(C)** the East Sea: the off-shore of coastal Korea (in February, April, August, and October for 2019–2020; r^2 = 0.494, p = 6.6 ×10^{-17}), and **(D)** Station ALOHA of the Hawaii Ocean Time-series measurements (2019–2020; r^2 = 0.035, p = 0.52; gray symbols for 2000–2019). The colored symbols indicate the sea surface temperature. The diagram displays the factors determining the correlations between $pCO_{2\,eq}$ and $pCO_{2\,in\ situ}$ (the x-axis and y-axis of **B–D**, respectively): the seasonal temperature extremes and the air–sea C flux regulate an overall slope of the correlation (combined angle of the dotted red and black arrows), and the biological metabolisms affect the magnitude of deviations (length of blue arrow), which affects the net slope.

variations; however, with increasing biological production, a decadal decrease in surface pCO_2 might occur as in other regions, including the southern Bering Sea and the peripheries of the Okhotsk Sea, where a substantial increase in primary production due to increasing input of nutrients *via* river and atmospheric deposition was reported (Takahashi et al., 2006).

Conclusion

Our results show that the biological perturbations are as significant as the thermal factors in affecting the pCO_2 dynamics in Korean coastal macroalgal habitats, although temperature changes have the greatest effect on the ocean C cycle. To fully characterize diverse ocean margin C systems, it is necessary to identify local processes involved and to quantify their impacts in ecosystems using highly resolved temporal and spatial data for coastal waters. Our results provide observational evidence for marked biological impacts on seawater carbonate dynamics in a coastal macroalgal habitat, and particularly their significant effects in the cooling period. Major effects of biological factors are likely to be found in many nutrient-rich marginal ocean waters, associated with rapidly increasing impact of human activity on coastal systems.

Data availability statement

The datasets presented in this study can be found in online repositories. The names of the repository/repositories and accession number(s) can be found below: Dryad (https://doi.org/10.5061/dryad.5qfttdz85) and GOA-ON (http://portal.goa-on.org/Explorer?action=oiw:mobile_platform:STS_667:observations:).

Author contributions

KL formulated the research question and designed the field survey. MK, HK, BJ, and I-SH supported the development of infrastructure for the C measurement system at the study site and conducted the field survey. J-MK and MK analyzed the data and J-MK and KL wrote the paper together. J-HK, T-HK, and KS measured dissolved oxygen, dissolved organic carbon, nutrients, respectively, and provided data for analysis. All authors contributed to the article and approved the submitted version.

Funding

This work was supported by the National Institute of Fisheries Science (R2022056), and the Korea Fisheries Resources Agency.

Acknowledgments

The 2 year-long field observations would not have been possible without critical logistics from the Korea Fisheries Resources Agency and support from POSCO. We thank Gyeong-Seok Lee, Min-Ji Park, and Seung-Ha Kim for sampling and analysis.

Conflict of interest

The authors declare that the research was conducted in the absence of any commercial or financial relationships that could be construed as a potential conflict of interest.

Publisher's note

Supplementary material

The Supplementary Material for this article can be found online at: https://www.frontiersin.org/articles/10.3389/fmars.2022.963193/full#supplementary-material

References

Borges, A. V. (2011). "Present day carbon dioxide fluxes in the coastal ocean and possible feedbacks under global change," in *Oceans and the atmospheric carbon content*. Eds. P. Duarte and J. M. Santana-Casiano (Dordrecht: Springer Netherlands), 47–77.

Cai, W.-J., Hu, X., Huang, W.-J., Murrell, M. C., Lehrter, J. C., Lohrenz, S. E., et al. (2011). Acidification of subsurface coastal waters enhanced by eutrophication. *Nat. Geosci.* 4 (11), 766–770. doi: 10.1038/ngeo1297

Cai, W.-J., Xu, Y.-Y., Feely, R. A., Wanninkhof, R., Jönsson, B., Alin, S. R., et al. (2020). Controls on surface water carbonate chemistry along north American ocean margins. *Nat. Commun.* 11 (1), 2691. doi: 10.1038/s41467-020-16530-z

Cao, Z., Yang, W., Zhao, Y., Guo, X., Yin, Z., Du, C., et al. (2019). Diagnosis of CO_2 dynamics and fluxes in global coastal oceans. *Natl. Sci. Rev.* 7 (4), 786–797. doi: 10.1093/nsr/nwz105

Choi, S. K., Oh, H.-J., Yun, S.-H., Lee, H. J., Lee, K., Han, Y. S., et al. (2020). Population dynamics of the 'Golden tides' seaweed, *Sargassum horneri*, on the southwestern coast of Korea: The extent and formation of golden tides. *Sustainability* 12 (7), 2903. doi: 10.3390/su12072903

Clayton, T. D., and Byrne, R. H. (1993). Spectrophotometric seawater pH measurements: total hydrogen ion concentration scale calibration of m-cresol purple and at-sea results. *Deep Sea Res. Part I: Oceanographic Res. Papers* 40 (10), 2115–2129. doi: 10.1016/0967-0637(93)90048-8

Dai, M., Cao, Z., Guo, X., Zhai, W., Liu, Z., Yin, Z., et al. (2013). Why are some marginal seas sources of atmospheric CO_2? *Geophysical Res. Lett.* 40 (10), 2154–2158. doi: 10.1002/grl.50390

Dickson, A. G., and Millero, F. J. (1987). A comparison of the equilibrium constants for the dissociation of carbonic acid in seawater media. *Deep Sea Res. Part A. Oceanographic Res. Papers* 34 (10), 1733–1743. doi: 10.1016/0198-0149(87)90021-5

Dickson, A. G., Sabine, C. L., and Christian, J. R. (Eds.) (2007). *Guide to best practices for ocean CO_2 measurements* (Sidney, BC, Canada: North Pacific Marine Science Organization).

Duarte, C. M., Gattuso, J.-P., Hancke, K., Gundersen, H., Filbee-Dexter, K., Pedersen, M. F., et al. (2022). Global estimates of the extent and production of macroalgal forests. *Global Ecol. Biogeography* 31 (7), 1422–1439. doi: 10.1111/geb.13515

Fong, M. B., and Dickson, A. G. (2019). Insights from GO-SHIP hydrography data into the thermodynamic consistency of CO_2 system measurements in seawater. *Mar. Chem.* 211, 52–63. doi: 10.1016/j.marchem.2019.03.006

Fortes, M. D., and Lüning, K. (1980). Growth rates of north Sea macroalgae in relation to temperature, irradiance and photoperiod. *Helgoländer Meeresuntersuchungen* 34 (1), 15–29. doi: 10.1007/BF01983538

Gao, X., Endo, H., Nagaki, M., and Agatsuma, Y. (2017). Interactive effects of nutrient availability and temperature on growth and survival of different size classes of *Saccharina japonica* (Laminariales, phaeophyceae). *Phycologia* 56 (3), 253–260. doi: 10.2216/16-91.1

Gruber, N. (2015). Carbon at the coastal interface. *Nature* 517 (7533), 148–149. doi: 10.1038/nature14082

Ikawa, H., and Oechel, W. C. (2015). Temporal variations in air-sea CO_2 exchange near large kelp beds near San Diego, California. *J. Geophysical Research: Oceans* 120 (1), 50–63. doi: 10.1002/2014JC010229

Kakinuma, M., Coury, D. A., Kuno, Y., Itoh, S., Kozawa, Y., Inagaki, E., et al. (2006). Physiological and biochemical responses to thermal and salinity stresses in a sterile mutant of ulva pertusa (Ulvales, chlorophyta). *Mar. Biol.* 149 (1), 97–106. doi: 10.1007/s00227-005-0215-y

Kim, J.-M., Lee, K., Han, I.-S., Lee, J.-S., Choi, Y.-H., Lee, J. H., et al. (2020). Anthropogenic nitrogen-induced changes in seasonal carbonate dynamics in a productive coastal environment. *Geophysical Res. Lett.* 47 (17), e2020GL088232. doi: 10.1029/2020GL088232

Krause-Jensen, D., and Duarte, C. M. (2016). Substantial role of macroalgae in marine carbon sequestration. *Nat. Geosci.* 9 (10), 737–742. doi: 10.1038/ngeo2790

Kubo, A., Maeda, Y., and Kanda, J. (2017). A significant net sink for CO_2 in Tokyo bay. *Sci. Rep.* 7 (1), 44355. doi: 10.1038/srep44355

Laruelle, G. G., Landschützer, P., Gruber, N., Tison, J. L., Delille, B., and Regnier, P. (2017). Global high-resolution monthly pCO_2 climatology for the coastal ocean derived from neural network interpolation. *Biogeosciences* 14 (19), 4545–4561. doi: 10.5194/bg-14-4545-2017

Laruelle, G. G., Lauerwald, R., Pfeil, B., and Regnier, P. (2014). Regionalized global budget of the CO_2 exchange at the air-water interface in continental shelf seas. *Global Biogeochemical Cycles* 28 (11), 1199–1214. doi: 10.1002/2014GB004832

Lee, K., Chris, S., Tanhua, T., Kim, T.-W., Feely, R., and Kim, H.-C. (2011). Roles of marginal seas in absorbing and storing fossil fuel CO_2. *Energy Environ. Sci.* 4, 1133–1146. doi: 10.1039/C0EE00663G

Lee, K., Kim, T.-W., Byrne, R. H., Millero, F. J., Feely, R. A., and Liu, Y.-M. (2010). The universal ratio of boron to chlorinity for the north pacific and north Atlantic oceans. *Geochimica Cosmochimica Acta* 74 (6), 1801–1811. doi: 10.1016/j.gca.2009.12.027

Lee, K., Kim, J.-M., Lee, G.-S., Lee, E., Jeong, J.-Y., Lee, J., et al. (2022). Persistent continental shelf carbon sink at the ieodo ocean research station in the northern East China Sea. *Front. Mar. Sci.* 9. doi: 10.3389/fmars.2022.919249

Lee, K., and Millero, F. J. (1995). Thermodynamic studies of the carbonate system in seawater. *Deep Sea Res. Part I: Oceanographic Res. Papers* 42 (11), 2035–2061. doi: 10.1016/0967-0637(95)00077-1

Lee, K., Millero, F. J., and Campbell, D. M. (1996). The reliability of the thermodynamic constants for the dissociation of carbonic acid in seawater. *Mar. Chem.* 55 (3), 233–245. doi: 10.1016/S0304-4203(96)00064-3

Li, H., Moon, H., Kang, E. J., Kim, J.-M., Kim, M., Lee, K., et al. (2022). The diel and seasonal heterogeneity of carbonate chemistry and dissolved oxygen in three types of macroalgal habitats. *Front. Mar. Sci.* 9. doi: 10.3389/fmars.2022.857153

Lueker, T. J., Dickson, A. G., and Keeling, C. D. (2000). Ocean pCO_2 calculated from dissolved inorganic carbon, alkalinity, and equations for K_1 and K_2: Validation based on laboratory measurements of CO_2 in gas and seawater at equilibrium. *Mar. Chem.* 70 (1), 105–119. doi: 10.1016/S0304-4203(00)00022-0

Macreadie, P. I., Anton, A., Raven, J. A., Beaumont, N., Connolly, R. M., Friess, D. A., et al. (2019). The future of blue carbon science. *Nat. Commun.* 10 (1), 3998. doi: 10.1038/s41467-019-11693-w

Mehrbach, C., Culberson, C. H., Hawley, J. E., and Pytkowicx, R. M. (1973). Measurement of the apparent dissociation constants of carbonic acid in seawater at atmospheric pressure. *Limnology Oceanography* 18 (6), 897–907. doi: 10.4319/lo.1973.18.6.0897

Millero, F. J. (1995). Thermodynamics of the carbon dioxide system in the oceans. *Geochimica Cosmochimica Acta* 59 (4), 661–677. doi: 10.1016/0016-7037(94)00354-O

Nakawaki, T., Agatsuma, Y., and Taniguchi, K. (2001). Annual life cycle and productivity of the *Laminaria japonica* population in onagawa bay, northeastern Honshu, Japan. *Suisanzoshoku* 49 (4), 439–444.

Nellemann, C., Corcoran, E., Duarte, C., Valdes, L., Young, C., Fonseca, L., et al. (2009). "Blue carbon," in *A rapid response assessment* (Norway: United Nations Environment Programme).

Park, K.-S., Heo, K.-Y., Jun, K., Kwon, J.-I., Kim, J., Choi, J.-Y., et al. (2015). Development of the operational oceanographic system of Korea. *Ocean Sci. J.* 50 (2), 353–369. doi: 10.1007/s12601-015-0033-1

Park, G.-H., Lee, K., Tishchenko, P., Min, D.-H., Warner, M. J., Talley, L. D., et al. (2006). Large Accumulation of anthropogenic CO_2 in the East (Japan) Sea and its significant impact on carbonate chemistry. *Global Biogeochemical Cycles* 20 (4): GB4013. doi: 10.1029/2005GB002676

Serisawa, Y., Aoki, M., Hirata, T., Bellgrove, A., Kurashima, A., Tsuchiya, Y., et al. (2003). Growth and survival rates of large-type sporophytes of *Ecklonia cava* transplanted to a growth environment with small-type sporophytes. *J. Appl. Phycology* 15 (4), 311–318. doi: 10.1023/A:1025183100958

Signorini, S. R., Mannino, A., Najjar, R. G.Jr., Friedrichs, M. A. M., Cai, W.-J., Salisbury, J., et al. (2013). Surface ocean pCO_2 seasonality and sea-air CO_2 flux estimates for the north American east coast. *J. Geophysical Research: Oceans* 118 (10), 5439–5460. doi: 10.1002/jgrc.20369

Skriptsova, A., Khomenko, V., and Isakov, V. (2004). Seasonal changes in growth rate, morphology and alginate content in *Undaria pinnatifida* at the northern limit in the Sea of Japan (Russia). *J. Appl. Phycology* 16 (1), 17. doi: 10.1023/B:JAPH.0000019049.74140.61

Takahashi, T., Sutherland, S. C., Feely, R. A., and Wanninkhof, R. (2006). Decadal change of the surface water pCO_2 in the north pacific: A synthesis of 35 years of observations. *J. Geophysical Research: Oceans* 111, C07S05. doi: 10.1029/2005JC003074

Takahashi, T., Sutherland, S. C., Sweeney, C., Poisson, A., Metzl, N., Tilbrook, B., et al. (2002). Global sea–air CO_2 flux based on climatological surface ocean pCO_2, and seasonal biological and temperature effects. *Deep Sea Res. Part II: Topical Stud. Oceanography* 49 (9), 1601–1622. doi: 10.1016/S0967-0645(02)00003-6

Takahashi, T., Sutherland, S. C., Wanninkhof, R., Sweeney, C., Feely, R. A., Chipman, D. W., et al. (2009). Climatological mean and decadal change in surface ocean pCO_2, and net sea–air CO_2 flux over the global oceans. *Deep Sea Res. Part II: Topical Stud. Oceanography* 56 (8), 554–577. doi: 10.1016/j.dsr2.2008.12.009

Tominaga, H., Serisawa, Y., and Ohno, M. (2004). Seasonal changes in net production of the bladelets and size of the eproximal blade of *Ecklonia cava* in tosa bay, kochi prefecture. *Japanese J. Phycology* 52 (1), 13–19.

Wanninkhof, R. (2014). Relationship between wind speed and gas exchange over the ocean revisited. *Limnology Oceanography: Methods* 12 (6), 351–362. doi: 10.4319/lom.2014.12.351

Watanabe, K., Yoshida, G., Hori, M., Umezawa, Y., Moki, H., and Kuwae, T. (2020). Macroalgal metabolism and lateral carbon flows can create significant carbon sinks. *Biogeosciences* 17 (9), 2425–2440. doi: 10.5194/bg-17-2425-2020

Weiss, R. F. (1974). Carbon dioxide in water and seawater: the solubility of a non-ideal gas. *Mar. Chem.* 2 (3), 203–215. doi: 10.1016/0304-4203(74)90015-2

Zeebe, R. E., and Wolf-Gladrow, D. (2001). "Equilibrium," in *CO_2 in seawater: Equilibrium, kinetics, isotopes* (San Diego, CA, USA: Elsevier Science), 1–83.

Zhang, J.-Z., Wanninkhof, R., and Lee, K. (2001). Enhanced new production observed from the diurnal cycle of nitrate in an oligotrophic anticyclonic eddy. *Geophysical Res. Lett.* 28 (8), 1579–1582. doi: 10.1029/2000GL012065